

Global and regional functional connectivity maps of neural oscillations in focal epilepsy

Dario J. Englot,^{1,2,3} Leighton B. Hinkley,³ Naomi S. Kort,³ Brandon S. Imber,^{1,2}
Danielle Mizuri,³ Susanne M. Honma,³ Anne M. Findlay,³ Coleman Garrett,³
Paige L. Cheung,³ Mary Mantle,^{1,3} Phiroz E. Tarapore,^{1,2,3} Robert C. Knowlton,^{1,3,4}
Edward F. Chang,^{1,2,3} Heidi E. Kirsch^{1,3,4,*} and Srikantan S. Nagarajan^{1,3,*}

*These authors contributed equally to this work.

Intractable focal epilepsy is a devastating disorder with profound effects on cognition and quality of life. Epilepsy surgery can lead to seizure freedom in patients with focal epilepsy; however, sometimes it fails due to an incomplete delineation of the epileptogenic zone. Brain networks in epilepsy can be studied with resting-state functional connectivity analysis, yet previous investigations using functional magnetic resonance imaging or electrocorticography have produced inconsistent results. Magnetoencephalography allows non-invasive whole-brain recordings, and can be used to study both long-range network disturbances in focal epilepsy and regional connectivity at the epileptogenic zone. In magnetoencephalography recordings from presurgical epilepsy patients, we examined: (i) global functional connectivity maps in patients versus controls; and (ii) regional functional connectivity maps at the region of resection, compared to the homotopic non-epileptogenic region in the contralateral hemisphere. Sixty-one patients were studied, including 30 with mesial temporal lobe epilepsy and 31 with focal neocortical epilepsy. Compared with a group of 31 controls, patients with epilepsy had decreased resting-state functional connectivity in widespread regions, including perisylvian, posterior temporo-parietal, and orbitofrontal cortices ($P < 0.01$, t -test). Decreased mean global connectivity was related to longer duration of epilepsy and higher frequency of consciousness-impairing seizures ($P < 0.01$, linear regression). Furthermore, patients with increased regional connectivity within the resection site ($n = 24$) were more likely to achieve seizure postoperative seizure freedom (87.5% with Engel I outcome) than those with neutral ($n = 15$, 64.3% seizure free) or decreased ($n = 23$, 47.8% seizure free) regional connectivity ($P < 0.02$, chi-square). Widespread global decreases in functional connectivity are observed in patients with focal epilepsy, and may reflect deleterious long-term effects of recurrent seizures. Furthermore, enhanced regional functional connectivity at the area of resection may help predict seizure outcome and aid surgical planning.

1 UCSF Comprehensive Epilepsy Centre, University of California, San Francisco, California, USA

2 Department of Neurological Surgery, University of California, San Francisco, California, USA

3 Biomagnetic Imaging Lab, Department of Radiology and Biomedical Imaging, University of California, San Francisco, California, USA

4 Department of Neurology, University of California, San Francisco, California, USA

Correspondence to: Heidi Kirsch,
Biomagnetic Imaging Laboratory,
University of California, San Francisco,
513 Parnassus Avenue, S362,
San Francisco,
California, 94143-0628, USA
E-mail: Heidi.Kirsch@ucsf.edu

Keywords: epilepsy; functional connectivity; magnetoencephalography; outcome; surgery

Abbreviations: EEG = electroencephalography; FNE = focal neocortical epilepsy; MEG = magnetoencephalography; MTLE = mesial temporal lobe epilepsy; MRI = magnetic resonance imaging; RSFC = resting-state functional connectivity

Introduction

Epilepsy affects nearly 1% of the population, and seizures are refractory to medical treatment in about one-third of those individuals, leading to significant cumulative morbidity and increased mortality (Helmstaedter and Kockelmann, 2006; Choi *et al.*, 2008). In medically-refractory epilepsy, localization and surgical resection of the epileptogenic zone leads to seizure freedom in ~60–80% of patients with mesial temporal lobe epilepsy (MTLE) and about one-half of individuals with focal neocortical epilepsy (FNE) (Spencer and Huh, 2008; Englot *et al.*, 2013). This leaves substantial room for improvement in surgical outcomes, as seizure freedom is the single greatest predictor of quality-of-life in epilepsy (Macrodimitris *et al.*, 2011; Elliott *et al.*, 2012). Failures in the surgical treatment of epilepsy stem in part from an incomplete understanding of epileptic brain networks (Engel *et al.*, 2013), for most cases of failed epilepsy surgery involve incomplete delineation and resection of the epileptogenic zone from which seizures originate (Englot *et al.*, 2014a, b). Studying the networks involved in epilepsy may lead to enhanced techniques for localizing the true extent of the epileptogenic zone, an improved ability to predict surgical outcomes, and a better understanding of the effects that recurrent seizures have on various brain regions.

The pathophysiological underpinnings of seizure generation likely involve both abnormal brain structures and aberrant connections between these regions, resulting in large-scale network instability (Zhang *et al.*, 2011; Engel *et al.*, 2013; Jiruska *et al.*, 2013). Furthermore, aberrant brain network activity in epilepsy may contribute to devastating cognitive and neuropsychological sequelae that are frequently suffered in this disorder (Hermann *et al.*, 1997; Helmstaedter and Kockelmann, 2006; Laurent and Arzimanoglou, 2006). Abnormal network connections can be studied using resting-state functional connectivity (RSFC) analysis, which is performed between seizures (i.e. during the interictal period), avoiding the challenges associated with diagnostic recordings during the ictal period. However, functional connectivity studies in focal epilepsy have thus far produced inconsistent findings. The majority of these investigations have used functional MRI, and although some studies have found only decreased connectivity in focal epilepsy patients (Luo *et al.*, 2011; Voets *et al.*, 2012; Haneef *et al.*, 2014a; Maneshi *et al.*, 2014), others report increased connectivity in some networks juxtaposed by decreases in others (Liao *et al.*, 2010; Zhang *et al.*, 2010; Haneef *et al.*, 2014b; Luo *et al.*, 2014). In contrast, most RSFC studies using intracranial EEG have suggested predominantly increased connectivity involving the

epileptogenic zone and surrounding structures (Bettus *et al.*, 2008; Zaveri *et al.*, 2009; Bartolomei *et al.*, 2013; Holmes *et al.*, 2014). Differences in study techniques and analysis methods may contribute to the variability between these findings. For instance, functional MRI only allows indirect estimation of neuronal activity through blood oxygenation patterns, but does permit whole-brain connectivity analysis, whereas intracranial EEG provides direct neuronal recordings from the human brain, but only from the area of electrode coverage (Hyder and Rothman, 2012; Yuan *et al.*, 2012). More direct approaches to non-invasively map RSFC in focal epilepsy are needed, to examine both global connectivity throughout the entire brain, as well as regional connectivity related to the epileptogenic zone.

Magnetoencephalography (MEG) is a non-invasive technique for recording cerebral activity from the entire cortex through the detection of magnetic fields produced by electrophysiological signals (Guggisberg *et al.*, 2008; Burgess, 2011). It allows more direct measurement of neuronal activity at a significantly higher temporal resolution than functional MRI, and possesses high spatial resolution without signal deterioration by the skull and scalp that is present in scalp EEG (Guggisberg *et al.*, 2008; Burgess, 2011), MEG has been used to study RSFC in numerous brain disorders (Guggisberg *et al.*, 2008), including preoperative neurosurgical patients (Tarapore *et al.*, 2012), and recordings are already performed in many presurgical epilepsy patients to aid with the localization of interictal epileptic spikes (Stefan *et al.*, 2011; Englot *et al.*, 2015). Overall, MEG is well suited for non-invasive, whole-brain connectivity analysis in surgical epilepsy patients. A few groups have reported MEG-based functional connectivity analyses in epilepsy, although these have examined only global network organization without interrogating epileptogenic zone connectivity (Jeong *et al.*, 2014; van Dellen *et al.*, 2014). Another study investigated regional functional connectivity in epilepsy patients using MEG sensor-based calculations, but did not use metrics to identify the source of neural oscillations, and did not examine global connectivity maps (Wu *et al.*, 2014).

Recently, we have developed techniques to extract global functional connectivity maps across the whole brain from MEG recordings (Guggisberg *et al.*, 2008; Hinkley *et al.*, 2011; Tarapore *et al.*, 2013), and also generate regional functional connectivity maps to relate to behavioural outcomes (Guggisberg *et al.*, 2008; Martino *et al.*, 2011; Tarapore *et al.*, 2012). Here we report the first MEG-based study of RSFC in focal epilepsy to examine both whole brain connectivity and regional connectivity maps associated with the epileptogenic zone. We investigate 61 presurgical adult patients with medically-refractory MTLE

or FNE, comparing global connectivity maps in these individuals to matched controls, and relating connectivity alterations to duration and severity of epilepsy. Furthermore, we examine regional connectivity maps at the epileptogenic zone within individual patients, relating connectivity patterns to long-term seizure outcome after surgery.

Materials and methods

Subjects

Study subjects were selected from 310 patients referred for MEG as part of a clinical epilepsy evaluation at the University of California, San Francisco (UCSF) Biomagnetic Imaging Laboratory (BIL) between 1 June 2004 and 30 June 2013. Among these patients, 174 individuals also underwent surgical resection for medically-refractory epilepsy at our institution following MEG recordings, and were considered for inclusion in the study. Patients were then excluded for age <18 years at the time of MEG ($n = 45$), a history of resective brain surgery prior to MEG ($n = 24$), a lack of awake resting-state data (e.g. MEG performed only for task-based cortical mapping) ($n = 21$), extensive MEG artefact from a metallic object such as dental implants ($n = 4$), or postoperative follow-up of <1 year ($n = 8$). Finally, we excluded patients with a history of infiltrative and/or malignant brain tumour such as glioma ($n = 11$), but included those with pathology confirming a benign, non-infiltrating brain lesion, such as meningioma or cavernous malformation. The remaining 61 adults who received MEG followed by surgical resection for focal epilepsy, including 30 patients with MTL and 31 individuals with FNE, were included for analysis. Patients were 52.5% female, 82.0% right-handed, and mean age at the time of MEG recordings was 34.7 years (range 18–67 years). Thirty-one control subjects matched for age, gender and handedness were recorded during the same time period, and had no known history of epilepsy or other neurological disorder. Controls were 51.5% female, 83.9% right-handed, with mean age of 34.2 years (range 18–63 years). All procedures and subject consents in the study were in full compliance with UCSF clinical research policies, with research protocol approval by the UCSF Committee on Human Research.

MRI and MEG recordings

MRI studies were performed on a 3 T scanner (Excite, GE) using an 8-channel head coil. To provide anatomical head models for MEG analysis, a high-resolution 3D T_1 -weighted whole-brain volume was acquired using a fast spoiled gradient-recalled echo in a steady state inversion recovery (FSPGR-IR) sequence (repetition time 6.3 ms, echo time 1.5 ms, inversion time 400 ms, and flip angle 15°), slice thickness 1.0 mm, matrix size 256×256 , and field of view 230×230 mm with skin-to-skin coverage to include the nasion and preauricular points, as well as T_2 -weighted FLAIR images (echo time 126 ms, repetition time 10 s, and inversion time 2200 ms) with 220-mm field of view, 47–48 3.0-mm contiguous slices at a 256×256 matrix. All magnetic resonance images were interpreted by a board-certified attending neuroradiologist.

MEG recordings were performed inside a magnetically shielded room, with a 275 channel whole-head axial gradiometer system (VSM MedTech). Data were recorded from each patient in a passband of 0–75 Hz (600 Hz sample rate). A recording epoch of 1-min duration not limited by artefact or interictal epileptic spike activity, and with the subject awake but resting with eyes closed, was selected for subsequent analysis. We have previously shown that data stationarity is maintained within a 1-min period, but may be lost with longer intervals (Hinkley *et al.*, 2012). Also, prior studies in patients with various neurological disorders have suggested that 1 min of data is sufficient for the calculation of reliable functional connectivity maps (Guggisberg *et al.*, 2008). The MEG technician observed the subject during recordings, and noted 1-min data segments that consisted of periods of wakefulness with eyes closed. In addition, visual inspection of all MEG/EEG recordings was performed prior to analysis to ensure the absence of sleep rhythm components. The position of the head in the MEG relative to the MEG sensors was determined via indicator coils before and after each interval to ensure adequate sampling of the entire magnetic field. The data were bandpass filtered offline at 1–70 Hz.

Signal analysis algorithms

For the majority of connectivity analyses, alpha (8–12 Hz) activity was used, given that spectral power typically peaks in the alpha band during the awake resting state, and the alpha band contains the alpha peak, whereas other low spectral components, such as theta, do not contain prominent peaks. Also, we have previously found that the imaginary coherence analysis in the alpha band has the highest test-retest reliability (Hinkley *et al.*, 2012), and alpha-band imaginary coherence has been well-established as a measure of functional connectivity (Guggisberg *et al.*, 2008; Tarapore *et al.*, 2013). However, analyses were also performed using delta (1–4 Hz), theta (4–8 Hz), beta (12–30 Hz), or gamma (30–55 Hz) band activity where specified. An adaptive spatial filtering algorithm was used to reconstruct the electromagnetic neural activity at each brain voxel from the signal recorded by the entire MEG sensor array. The details of this algorithm are described elsewhere (Guggisberg *et al.*, 2008). In brief, the raw MEG data were bandpass filtered with a fourth-order Butterworth filter, and the spatial covariance matrix of the data was calculated from the entire recording of 1 min in duration. We also computed the lead-field matrix for each voxel in the brain, corresponding to the expected magnetic field pattern for a unit dipole in a particular orientation at a particular location. From the spatial covariance of the data and the lead-field matrix, a spatial weight matrix was then obtained for optimal estimation of the signal power in each voxel. The activity at each time in each voxel was then calculated as the linear combination of the spatial weighting matrix with the sensor data matrix. Thus, all sensors contributed in some degree to all voxel time series estimates from which we analysed functional connectivity. An orientation optimization step is built into our adaptive spatial filtering algorithms, and we have previously demonstrated that vector beam former and scalar beam former are identical with orientation optimization (Sekihara *et al.*, 2006). Source time courses were reconstructed by projecting sensor data with the estimated orientation.

We used the method of imaginary coherence to estimate functional connectivity, which overcomes estimation biases arising from seed-blur, crosstalk, or volume conduction, as described previously in detail (Nolte *et al.*, 2004; Guggisberg *et al.*, 2008; Sekihara *et al.*, 2011). Many commonly used measures of functional connectivity (e.g. coherence, phase locking value, synchronization likelihood) overestimate the magnitude of true connectivity because of common references and volume connection. By omitting the real component of coherence, which is dominated by similarities with zero time lags, we removed potentially spurious associations and limited the analysis to the imaginary component of coherence, which represents more realistic neural oscillatory interactions between brain areas occurring at non-zero time lags.

Functional connectivity maps

A 3D grid of voxels with an 8-mm spatial resolution covering the entire brain was created for each subject and recording. Source analysis was based on a multiple local sphere head model from coregistered structural 3D T₁-weighted FSPGR-IR magnetic resonance images. Although the sensitivity of MEG is significantly reduced for deeper sources, our analysis includes them and reports findings from deep structures subject to the same statistical tests as voxels in the rest of the brain. Alignment of structural and functional images was ensured by marking three prominent anatomical points (nasion and preauricular points) on the subject's head in the magnetic resonance images and localizing three fiducials attached to the same points before and after each MEG scan. MEG oscillation frequencies between 1 and 20 Hz (1–55 Hz for beta and gamma band analyses) were used for calculation of the spatial weighting matrix and the voxel time series. For calculation of imaginary coherence, the entire frequency bin of interest (usually alpha, 8–12 Hz) for each subject was averaged. The alpha peak, representing the point of greatest power density between 8 and 12 Hz during the resting state, was recorded for each subject. For imaginary coherence calculations, a frequency resolution of 1.17 Hz (512 frequency bins) was used. Imaginary coherence at each voxel of interest was estimated by averaging across all Fisher Z-transformed connections.

Two different connectivity maps were generated for each patient: (i) a patient-specific map (P-image) of global functional connectivity including all voxels throughout the brain, compared to that in control subjects; and (ii) a region-specific map (R-image) of regional connectivity including only voxels within the region of resection, compared to corresponding voxels in the homotopic contralateral region of the same patient. P-images were obtained by analysing all pairwise connections between voxels of 2 cm³ extension for each patient, resulting in ~30 000–60 000 voxel pairs in total depending on the individual's head size, and compared to the mean of those obtained from all control subjects. From the point of view of a single voxel, the P-image reflects the mean imaginary coherence between that voxel and every other voxel in the brain. Thus, a significant alteration in connectivity of that voxel suggests that its connectivity to the rest of the brain has changed. For group analysis of P-images, patients were assigned to one of four groups based on the side of resection (left or right) and type of focal epilepsy (MTLE or FNE). Each group was compared to healthy control subjects matched for age, gender, and handedness. Patient and subject P-images were spatially

normalized to the Montreal Neurological Institute atlas template according to the coregistered structural MRI, using the toolbox Statistical Parametric Mapping 8 (SPM8) for MATLAB (<http://www.fil.ion.ucl.ac.uk/spm/software/spm8/>). In summary, the connections calculated for R-images comprise a subset of the connections used for P-images, although P-images and R-images differ by which voxels are used as control. For R-images, contralateral homotopic voxels in the same patient are used as control, while in P-images, comparison is made between patients and spatially matched voxels in control subjects.

Regional connectivity maps (R-images) were generated by analysing all connections within the area of resection and a centred, equally spaced, whole-brain grid of each fourth voxel within the entire set of voxels. The mean connection strength was used to relate voxels in the resection volume with those in the whole-head grid. Also, voxels in the resection volume were not excluded from the analysis, but have only a small contribution to imaginary coherence calculations, because (i) voxels in the resection volume are nearby, and thus have low imaginary coherence; and (ii) there are many fewer voxels in the resection volume than in the rest of the brain. For the whole-brain grid, every fourth voxel is used for reasons of computational efficiency, and we have previously demonstrated that this does not influence the resultant calculations (Guggisberg *et al.*, 2008). The region for analysis was individually selected and drawn for each patient to represent the entire area of surgical resection. The limits of the resection area were defined by examination of the postoperative MRI, in addition to review of the operative report. Resections were planned to include the presumed epileptogenic zone, as determined preoperatively by the comprehensive clinical epilepsy team, and to avoid eloquent cortex. For MTLE cases, anatomic anterior temporal lobectomy was performed including both mesial structures (hippocampus, amygdala, entorhinal cortex) and the lateral cortex of the anterior temporal lobe, and thus these regions were included in the regional analysis. For FNE cases involving resection of a focal discrete lesion devoid of functional neural elements (e.g. ganglioglioma or cavernous malformation), a 1–2 cm rim of cortex surrounding the lesion was also included in the regional analysis, as seizure onsets were expected to involve perilesional parenchyma. As an internal control, the imaginary coherence was also calculated for connections between homotopic voxels contralateral to the side of resection of resection using the same whole-brain voxel grid.

Evaluation of clinical data and seizure outcomes

For all patients, we retrospectively reviewed outpatient and inpatient provider notes, diagnostic and laboratory reports, operative records, and pathology reports. Clinical and demographic data including patient gender, age, handedness, surgical history, the results of neuroimaging or electrographic diagnostic studies, and the side and region of surgery were recorded. Details regarding patients' epilepsy history and seizure semiology, including epilepsy duration, seizure type and frequency, were obtained from preoperative assessments by epileptologists. Based on epileptologist assessment, the seizure types investigated included consciousness-impairing seizures (comprising both focal dyscognitive seizures and secondarily

generalized tonic-clonic seizures) as well as consciousness-sparing focal seizures. Surgical decisions were made by a comprehensive team of epileptologists, neurosurgeons, neuropsychologists, neuroradiologists, and other practitioners. Surgical specimens were analysed by neuropathologists. Seizure outcome was determined by the latest patient follow-up using the Engel classification system, with Engel class I outcome (seizure freedom) used to signify postoperative freedom from all disabling seizures, and Engel class II–IV outcomes signifying varying degrees of persistent seizures (Engel *et al.*, 1993).

Statistical analyses

Group analysis between P-images for MTLE or FNE patients and the control group was performed with voxel-wise *t*-tests, corrected for multiple comparisons with a 5% False Discovery Rate (FDR) modified for dependency. All normalized P-image (whole-brain connectivity map) voxels of epilepsy patients with Z-transformed connectivity estimates greater than or less than the 95% confidence interval (CI) of the values of control subjects, after FDR correction, were considered significantly abnormal. Mean imaginary coherence of all voxels in the brain was calculated as an estimate of global functional connectivity. Individual unpaired *t*-tests with Bonferroni correction for multiple comparisons were used to compare global connectivity in each frequency band between MTLE patients, FNE patients, and controls. Factors were examined for potential association with mean imaginary coherence via multivariate analysis using a generalized step-wise linear regression model. Generalized linear regression was used to generate voxel-wise maps of connectivity as a function of epilepsy duration or seizure frequency across all patients. For R-images (regional connectivity maps), patients were designated as having increased connectivity ($t > 0.2$), decreased connectivity ($t < -0.2$), or neutral connectivity ($-0.2 > t > 0.2$), based on mean *t*-scores across all voxel-wise comparisons of imaginary coherence in the region of analysis versus contralateral voxels. Regional connectivity pattern was related to postoperative seizure outcome (Engel I versus Engel II–IV outcome) and neurological outcome (presence versus absence of new postoperative neurological deficit) with individual chi-square tests. All statistical analyses were performed using SPSS 20 (IBM) and statistical significance was assessed at $P < 0.05$, unless otherwise specified.

Results

Global and regional RSFC maps were analysed in 61 patients who underwent resection for medically-refractory focal epilepsy, including 30 individuals with MTLE and 31 patients with FNE. Patient demographics and epilepsy characteristics are summarized in Table 1.

Widespread decreased connectivity in patients with epilepsy compared to controls

To generate whole-brain global functional connectivity maps (P-images) for patients versus control subjects,

Table 1 Patient characteristics

Characteristic	
Age, years	34.7 ± 1.5
Gender	
Male	29 (47.5)
Female	32 (52.5)
Handedness	
Right	50 (82.0)
Left	11 (18.0)
Duration of epilepsy, years	19.0 ± 1.8
Region of epilepsy	
MTLE	30 (49.2)
FNE	31 (50.8)
Lateral temporal	15 (24.6)
Frontal	8 (13.1)
Parietal	3 (4.9)
Occipital	1 (1.6)
Multiple lobes	4 (6.6)
Seizure frequency, number per week, total	7.1 ± 1.2
Consciousness-impairing	5.0 ± 0.9
Consciousness-sparing	2.1 ± 0.7
Anti-epileptic drugs failed, number	4.4 ± 0.3
Current anti-epileptic drugs, number	2.0 ± 0.1
History of generalized seizures	
Yes	37 (61)
No	24 (39)
MRI findings	
Abnormal	51 (83.6)
Normal	10 (16.4)
Side of surgery	
Left	35 (57.4)
Right	26 (42.6)
Pathology	
Mesial temporal sclerosis	19 (31.1)
Gliosis only	17 (27.9)
Focal cortical dysplasia	11 (18.0)
Tumour	9 (14.8)
Other	5 (8.2)

Data are n (%) for categorical variables or mean ± SEM for continuous variables. $n = 61$ patients.

alpha-band imaginary coherence was calculated between all reconstructed brain voxels using resting-state MEG recordings. Group analysis of MTLE patients revealed decreased RSFC compared to controls in widespread regions (Fig. 1). In patients with left-sided MTLE, decreased connectivity was observed in the right lateral frontal, bilateral posterior temporal, bilateral parieto-occipital, and right perisylvian neocortices. Decreased connectivity was also seen in deep structures such as the basal forebrain, basal ganglia, anterior thalamus, posterior orbitofrontal cortex, posterior cingulate/precuneus, and right anterior insula, subject to the same statistical analyses (Fig. 1A). Similar large decreases in connectivity were seen in patients with right MTLE, affecting the bilateral perisylvian region, lateral frontal neocortex, basal forebrain, basal ganglia, anterior thalamus, orbitofrontal cortex, and insula (Fig. 1B). No

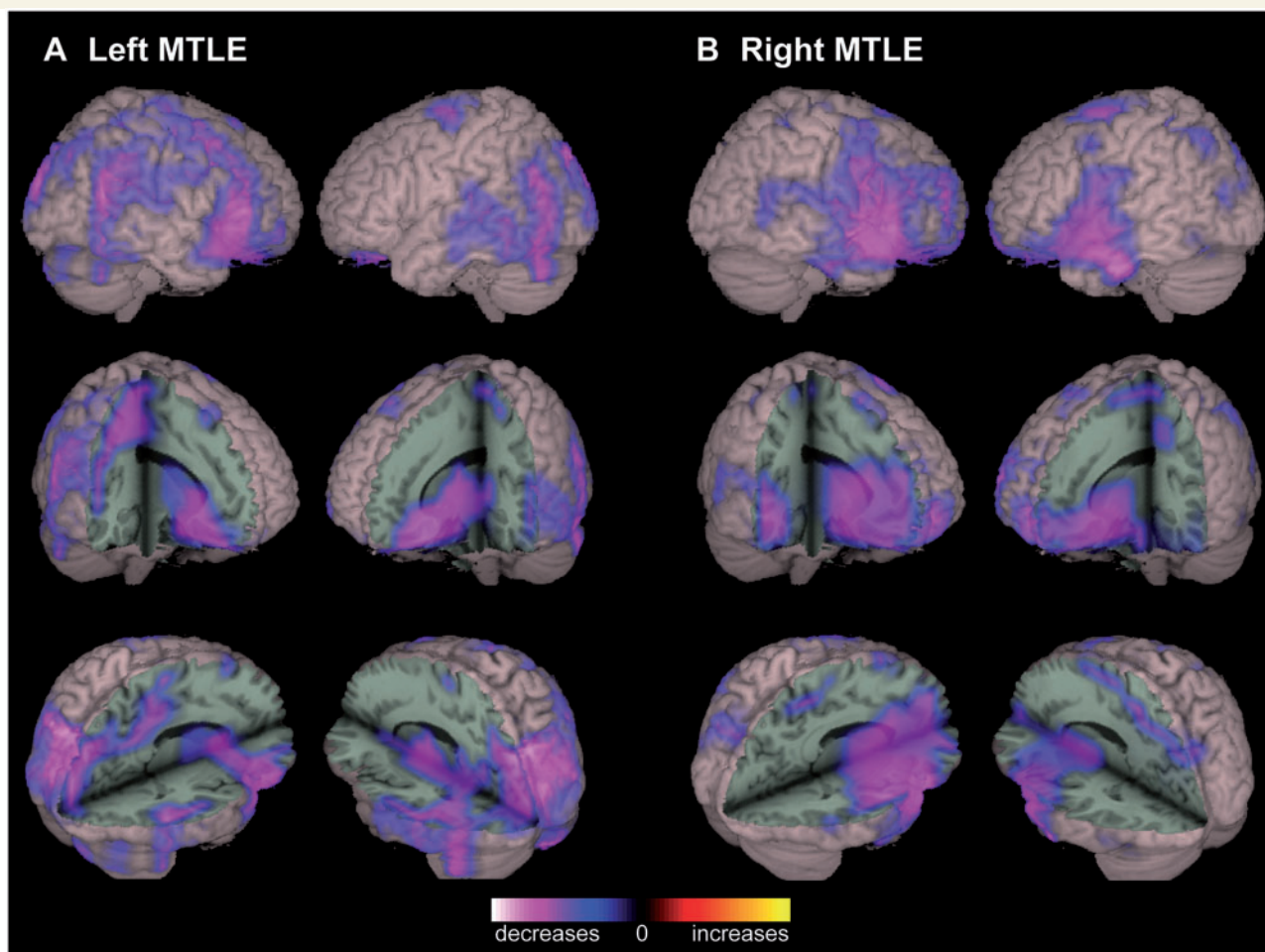


Figure 1 Decreased functional connectivity in patients with MTLE. (A) Compared to control subjects, patients with left MTLE demonstrate decreased RSFC in widespread regions including right lateral frontal, bilateral posterior temporal, bilateral parieto-occipital, and right perisylvian neocortex, as well as basal forebrain, basal ganglia, anterior thalamus, posterior orbitofrontal cortex, posterior cingulate/precuneus, and right anterior insula. (B) Similar connectivity decreases are observed in patients with right MTLE, most prominent in the perisylvian and lateral frontal neocortex, as well as the basal forebrain, basal ganglia, anterior thalamus, orbitofrontal cortex, and insula. In both left and right MTLE, no regions of increased connectivity are observed, and significant connectivity alterations are not seen in the mesial temporal structures. Connectivity maps represent *t*-tests (threshold $P < 0.01$, FDR-corrected) of alpha-band imaginary coherence in patients with left ($n = 18$) or right ($n = 12$) MTLE compared to controls, overlaid on a 3D-rendered template brain.

areas of increased connectivity were observed, and no significant connectivity alterations were noted in the mesial temporal structures of MTLE patients versus controls. Whole-brain RSFC maps in FNE patients also revealed various regions of decreased connectivity compared to controls, including the perisylvian, parieto-occipital, and posterior temporal neocortex, and subcortically in the basal forebrain, basal ganglia, and anterior thalamus (Fig. 2).

Given consistently decreased connectivity in epilepsy patients versus controls, the mean of the global functional connectivity maps was calculated across all brain voxels in each subject, to create a single 'global mean connectivity' metric with which to relate other factors of interest. Overall, global mean alpha-band connectivity was significantly decreased in patients with MTLE [0.044 ± 0.006

(mean \pm SEM), arbitrary units] and FNE (0.043 ± 0.007) compared to controls (0.049 ± 0.004) ($P < 0.01$ for each comparison), but there was no significant difference in connectivity between MTLE and FNE patients ($P = 0.48$) (*t*-tests with Bonferroni correction). The alpha peak frequency from resting-state power spectra was also measured for all subjects, and a lower alpha peak frequency was observed in individuals with MTLE [9.6 ± 0.1 Hz (mean \pm SEM)] or FNE (9.8 ± 0.1) compared to controls (10.2 ± 0.1 Hz) ($P < 0.05$ for each comparison), but no difference in alpha peak frequency was seen between MTLE and FNE patients ($P = 0.3$) (*t*-tests with Bonferroni correction). Mean imaginary coherence was also compared across subjects in the delta, theta, beta, and gamma frequency bands, revealing decreased global mean connectivity in epilepsy patients

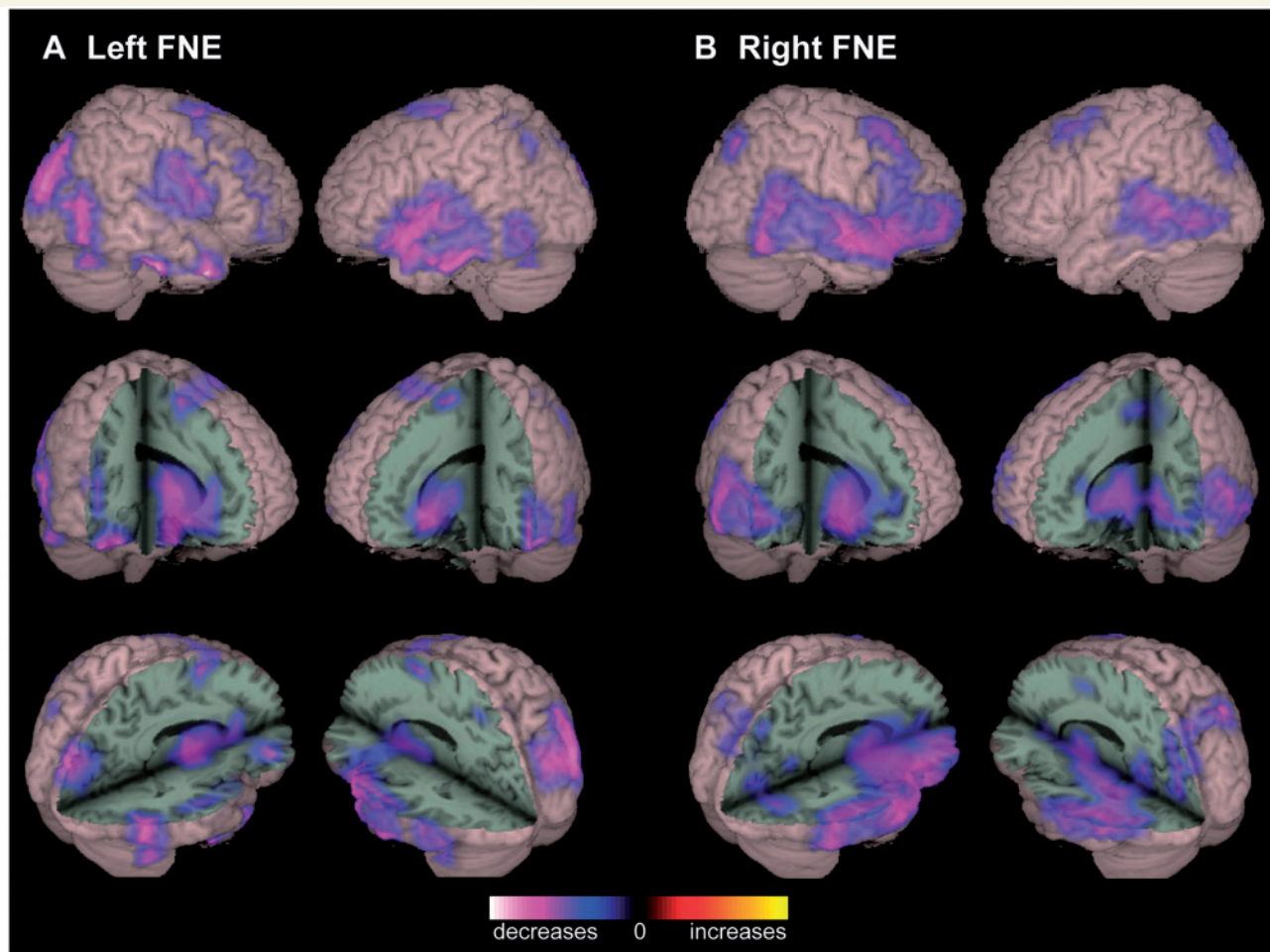


Figure 2 Decreased functional connectivity in patients with FNE. (A) In left FNE patients, decreased RSFC is observed in several locations compared to controls, including left perisylvian, right parieto-occipital, and bilateral posterior temporal neocortex. Subcortical decreases are seen in the basal forebrain, basal ganglia, and anterior thalamus. (B) Decreased connectivity is also observed in patients with right FNE, including right perisylvian and inferior frontal, as well as posterior temporal, lateral frontal, and parieto-occipital neocortex, as well as the anterior thalamus and right insula. No regions of significantly increased connectivity are seen in left or right FNE. Connectivity maps represent *t*-tests (threshold $P < 0.01$, FDR-corrected) of alpha-band imaginary coherence in patients with left ($n = 17$) or right ($n = 14$) FNE compared to controls, overlaid on a 3D-rendered template brain.

across all bands except gamma (Fig. 3). Overall, these results suggest marked disruption in global RSFC in patients with focal epilepsy.

Decreased global mean functional connectivity is related to duration and severity of epilepsy

Various factors were then interrogated for potential association with global mean RSFC (i.e. alpha-band imaginary coherence), including both categorical (gender, handedness, side of surgery, MTL or FNE, and lesional versus non-lesional epilepsy) and continuous variables (age, duration of epilepsy, frequency of consciousness-impairing and consciousness-sparing seizures, and numbers of current and

previous anti-epileptic medications). Seizure frequency was stratified by seizures which impair consciousness versus those that spare consciousness, given previous evidence of impaired cortical function with consciousness-impairing seizures (Englot and Blumenfeld, 2009). Multivariate analysis revealed that duration of epilepsy (Fig. 4A) and frequency of consciousness-impairing seizures (Fig. 4B) were negatively associated with global connectivity, while other variables showed no significant relationship. Furthermore, voxel-wise maps of RSFC regressed by epilepsy duration (Fig. 4C) or seizure frequency (Fig. 4D) revealed a negative relationship to connectivity in the frontal lobes, particularly the left prefrontal and orbitofrontal cortex. These findings suggest that RSFC alterations in focal epilepsy are quantitatively related to severity of illness.

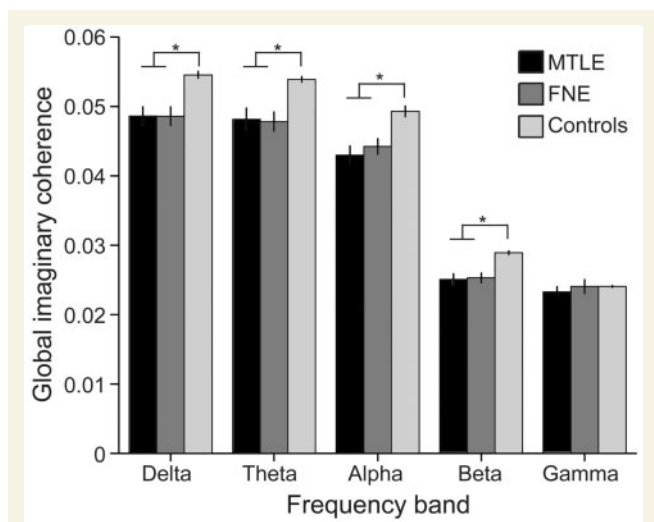


Figure 3 Global mean functional connectivity is decreased in patients with focal epilepsy. Global functional connectivity, estimated by mean imaginary coherence across all brain voxels, is significantly decreased in epilepsy patients in the delta (1–4 Hz), theta (4–8 Hz), alpha (8–12 Hz), and beta (12–30 Hz) frequency bands compared to controls. No difference in global connectivity is observed in the gamma (30–55 Hz) band. Data are mean \pm SEM (arbitrary units). * $P < 0.05$, t -tests with Bonferroni correction.

Regional connectivity maps of the area of resection predict seizure outcome

To address the question of how functional connectivity at the epileptogenic zone differs from other brain regions within individual patients, regional connectivity maps (R-images) were generated for each patient, measuring imaginary coherence of the area of resection. Specifically, these maps investigate long-range connectivity between the region of resection and the rest of the brain, compared to homotopic voxels in the non-epileptogenic hemisphere. Figure 5 depicts an example regional connectivity map of a 34-year-old right-handed female with MTLE, showing increased connectivity in the right mesial temporal lobe, with a smaller area of diminished connectivity in the lateral temporal cortex. In contrast, Fig. 6 displays a regional connectivity map of a 55-year-old right-handed female with FNE from a right frontal meningioma, in which only decreases in connectivity are seen surrounding the lesion. Overall, connectivity at the resection region was predominantly increased (mean voxel t -score > 0.2) in 24 patients (39.3%), decreased ($t < 0.2$) in 23 patients (37.7%), and neutral ($-0.2 < t < 0.2$) in 15 individuals (24.5%).

Regional connectivity at the resection area was also related to postoperative seizure outcome. After mean (\pm SEM) postoperative follow-up of 2.9 ± 0.4 years (range 1–10 years), 41 (67.2%) patients were free of disabling

seizures (Engel class I outcome), while 20 (32.8%) individuals continued to experience seizures (Engel class II–IV outcome). As shown in Fig. 7, seizure freedom was achieved in 87.5% of patients with increased connectivity at the region of resection, but in only 64.3% of individuals with neutral connectivity, and in 47.8% of patients with decreased connectivity ($\chi^2 = 8.5$, $P = 0.015$).

Finally, no incidences of perioperative mortality or severe morbidity were observed, but 10 (16.4%) patients did have a new or worsened neurological deficit immediately after surgery. Postoperative neurological deficits included eight patients with transient expressive or receptive aphasia, one individual with slight hand clumsiness and proprioceptive deficit, one patient with both transient mild aphasia and right superior quadrantanopia, and a case of expected dense hemianopia after occipital resection. In two additional individuals with hemiparesis, the deficit was stable compared to preoperative baseline. No relationship was detected between the presence of a new neurological deficit and regional connectivity pattern at the resection region ($\chi^2 = 2.2$, $P = 0.33$).

Discussion

The present study is the first to use MEG-based brain-space RSFC analysis to examine both global functional connectivity maps in focal epilepsy, as well as regional connectivity maps related to the epileptogenic zone, allowing novel insights into the impact of epilepsy on resting-state oscillatory networks. In both MTLE and FNE patients, we observed decreased connectivity in widespread regions compared to controls. Although most analyses measured connectivity in the alpha-band, global connectivity reductions were also seen in all other frequency bands with the exception of gamma, although gamma-band imaginary coherence has been shown to have the lowest test-retest probability (Hinkley *et al.*, 2012). We observed larger connectivity decreases in patients with a longer duration of epilepsy or higher frequency of consciousness-impairing seizures, suggesting a quantitative relationship between disease severity and RSFC alterations. While regional connectivity patterns differed between patients, increased connectivity of the resection site significantly predicted seizure freedom after surgery. Overall, our results suggest that MEG-based RSFC analysis can provide useful information related to the impact of disease on brain networks, and may aid in surgical planning and outcome prediction in focal epilepsy.

Most prior studies of RSFC in epilepsy have been performed using functional MRI, with several showing widespread decreases in connectivity in focal epilepsy patients versus controls (Luo *et al.*, 2011; Voets *et al.*, 2012; Haneef *et al.*, 2014a; Maneshi *et al.*, 2014). However, some functional MRI studies have also noted local increases in connectivity related to the epileptogenic zone, alongside decreases in long-range connectivity (Liao *et al.*, 2010; Haneef *et al.*, 2014b; Luo *et al.*, 2014). Regional increases

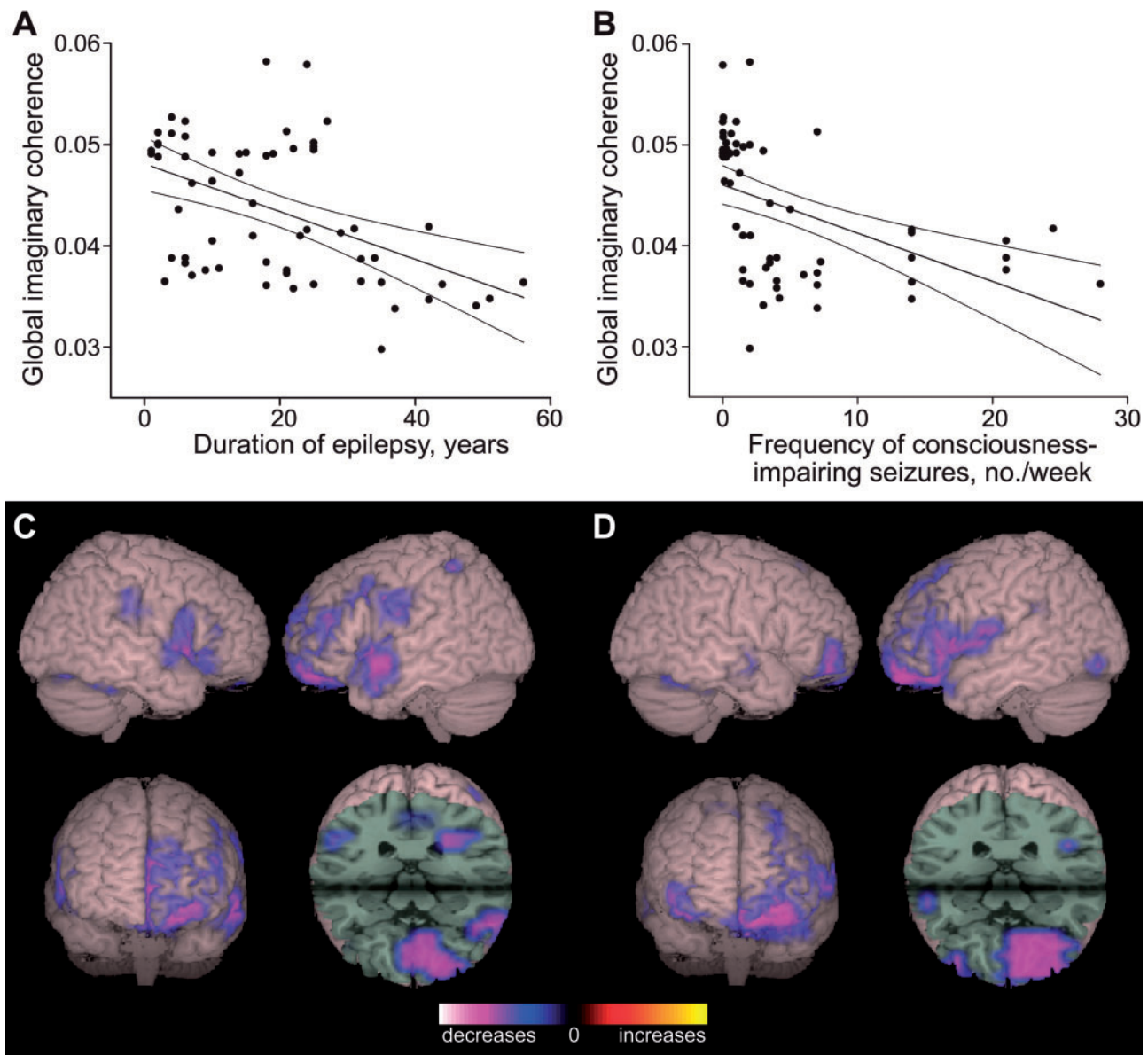


Figure 4 Longer epilepsy duration and higher seizure frequency are associated with decreased functional connectivity. (A) Global functional connectivity, estimated by mean imaginary coherence across all brain voxels, is negatively related to epilepsy duration in patients with focal epilepsy ($R^2 = 0.229$, $P < 0.001$). (B) A negative relationship is also observed between the frequency of consciousness-impairing seizures and mean imaginary coherence ($R^2 = 0.121$, $P < 0.01$). For A and B, units are arbitrary, $n = 61$ patients with MTLE and FNE, and line of best fit is shown with 95% CI. (C and D) Regional maps of RSFC regressed by epilepsy duration (C) or seizure frequency (D) reveal a negative relationship to connectivity in the frontal lobes, particularly left prefrontal and orbitofrontal cortex. For C and D, connectivity maps represent linear regression analysis (threshold $P < 0.01$, FDR-corrected) of alpha-band imaginary coherence in all 61 patients, overlaid on a 3D-rendered template brain.

in connectivity are supported in part by intracranial EEG data, which show predominantly elevated connectivity in relation to the epileptogenic zone and surrounding structures (Bettus *et al.*, 2008; Zaveri *et al.*, 2009; Bartolomei *et al.*, 2013; Holmes *et al.*, 2014). However, intracranial EEG studies are inherently limited to the area of electrode coverage, and thus do not permit whole-brain connectivity analysis. MEG provides a unique opportunity

to non-invasively study both whole-brain and regional connectivity, using a more direct measurement of neuronal activity than functional MRI (Guggisberg *et al.*, 2008; Burgess, 2011). Our results build upon previous studies, and suggest that focal epilepsy leads to decreased long-range connectivity, but is associated with increased regional connectivity at the epileptogenic zone in certain patients.

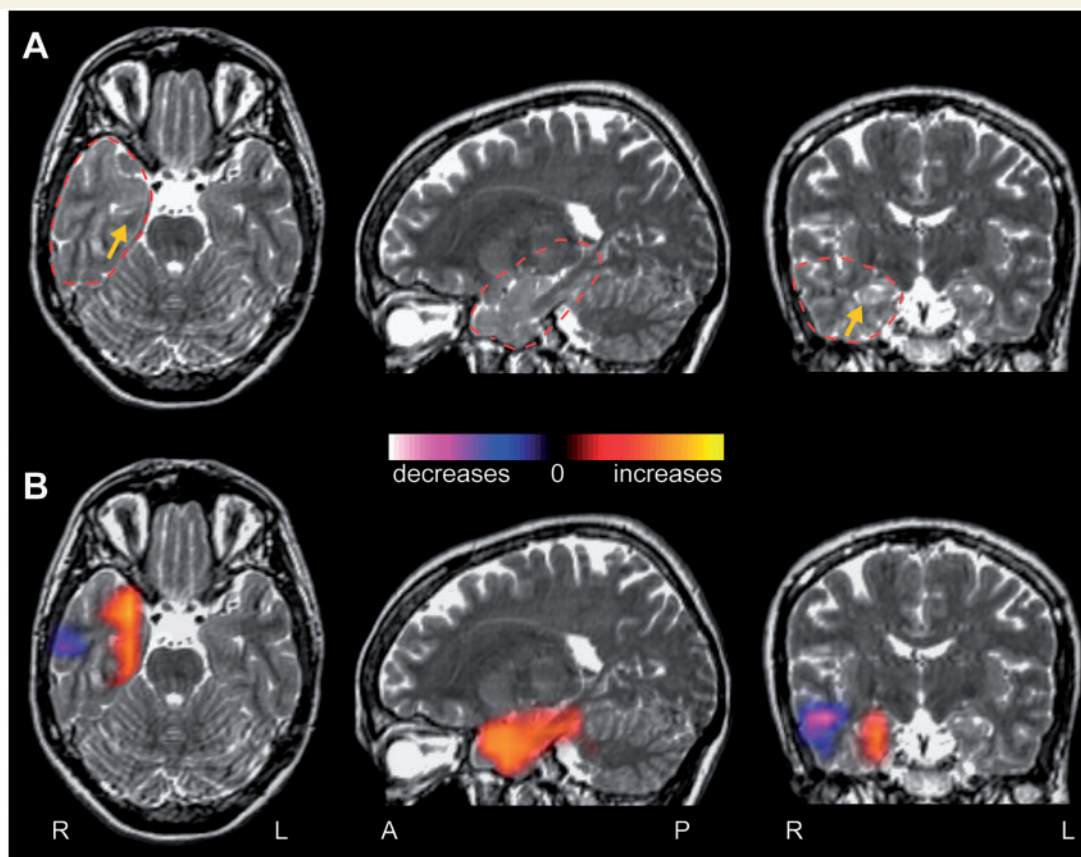


Figure 5 Example patient with increased connectivity at the resection region. (A) T₂-weighted MRI images from a 34-year-old right-handed female suffering from intractable focal dyscognitive and secondarily-generalized seizures for 21 years. The right anterior hippocampus shows slight T₂ signal hyperintensity and blurred cytoarchitecture compared to the left side, suggestive of mesial temporal sclerosis (yellow arrow). Dashed red line represents region used for connectivity analysis. (B) A regional functional connectivity map (R-image) shows increased connectivity between the mesial temporal lobe and the rest of the brain, compared to corresponding voxels in the contralateral hemisphere. A smaller area of decreased connectivity is also seen in the lateral temporal cortex.

How might recurrent seizures lead to decreased long-range connectivity? While our current analyses examine network status during the interictal state, divergent effects of seizures on local versus long-range networks have also been described during the ictal period. Intracranial EEG and single positron emission computed tomography (SPECT) studies in patients with MTLE have shown that during focal limbic seizures, fast spike activity and increased cerebral blood flow in the mesial temporal lobe are in stark contrast with slow wave activity and decreased cerebral blood flow in the distal fronto-parietal neocortices (Blumenfeld *et al.*, 2004a, b; Englot *et al.*, 2010). Furthermore, rat models of focal seizures have shown increased neuronal activity, cerebral blood flow and oxygen consumption at the epileptogenic zone during seizure activity that are juxtaposed with ictal decreases in all of these parameters in remote cortical regions (Englot *et al.*, 2008). These long-range neocortical effects of focal seizures appear to involve ictal recruitment of the thalamus, septal nuclei, and other subcortical regions, and can be prevented if seizure activity remains confined to the limbic structures (Englot *et al.*, 2009). Together, these previous human and

rodent studies suggest that long-range neocortical inhibition during focal seizures may result from aberrant activity in subcortical activating systems—a phenomenon termed ‘the network inhibition hypothesis’ (Englot and Blumenfeld, 2009; Danielson *et al.*, 2011). It is possible that ictal network inhibition represents a form of long-range surround inhibition that prevents seizure propagation to distal brain regions.

Over time, recurrent seizures likely result in diminished long-range connectivity between subcortical and cortical structures, which may in turn contribute to known deleterious effects of epilepsy including grey matter atrophy, cortical hypometabolism, neuropsychological sequelae, and cognitive impairment (Hermann *et al.*, 1997; Diehl *et al.*, 2003; Bonilha *et al.*, 2006; Helmstaedter and Kockelmann, 2006; Laurent and Arzimanoglou, 2006). This hypothesis is supported by the quantitative relationship we observed between epilepsy duration and decreased global connectivity in the present study. We also observed alpha slowing in patients compared to controls, which has previously been described in individuals with neurocognitive disorders (Larsson and Kostov, 2005; Garces *et al.*, 2013). Next,

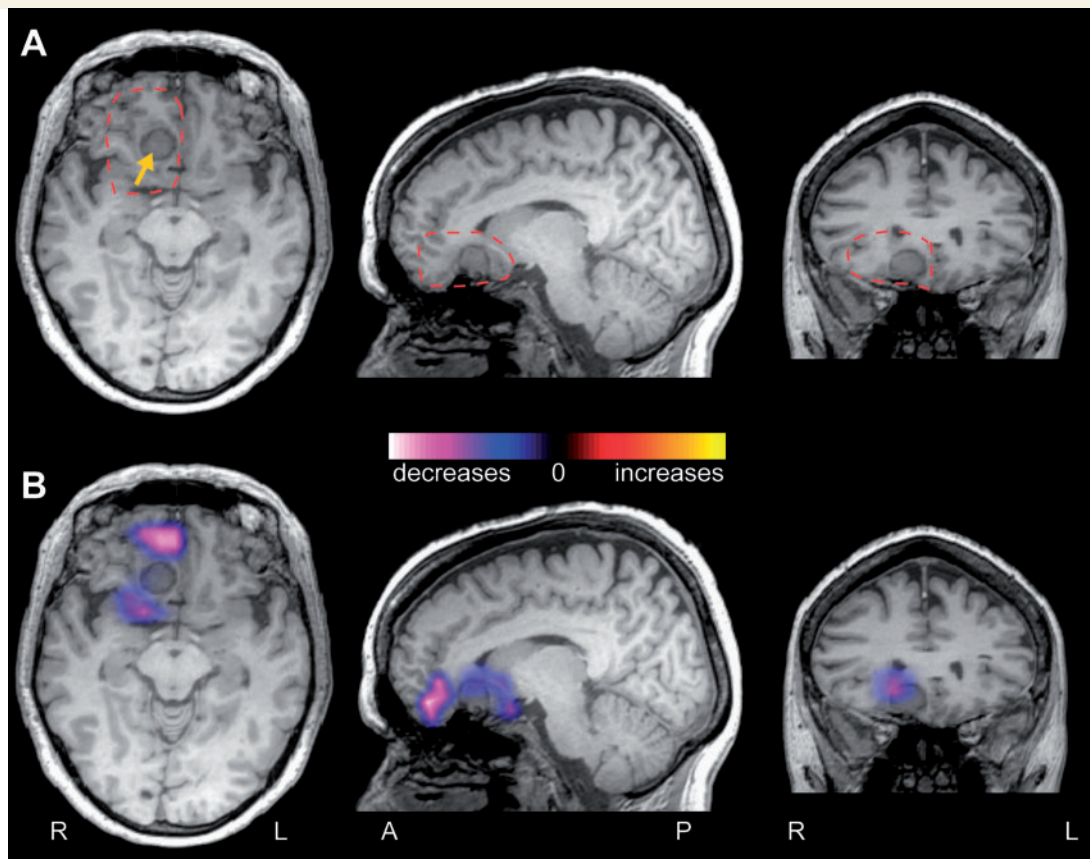


Figure 6 Example patient with decreased connectivity at the resection region. (A) T₁-weighted MRI images from a 55-year-old right-handed female with a 7-year history of intractable focal dyscognitive and secondarily-generalized seizures. An extra-axial lesion is at the medial floor of the right anterior fossa, consistent with meningioma (yellow arrow). Dashed red line represents region used for connectivity analysis. (B) A regional functional connectivity map (R-image) shows decreased connectivity between cortex surrounding the lesion and the rest of the brain, compared to corresponding voxels in the contralateral hemisphere. No areas of increased connectivity are seen.

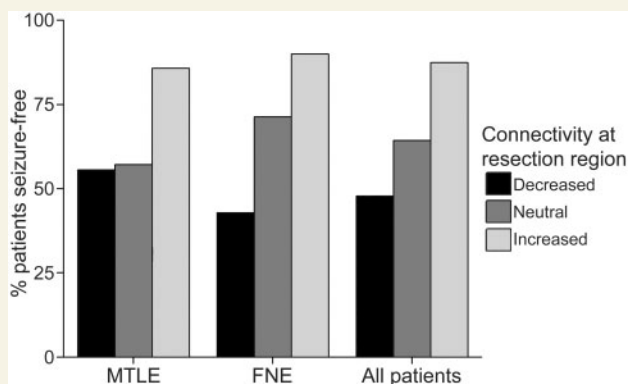


Figure 7 Increased connectivity at the resection region is associated with seizure freedom after surgery.

Postoperative seizure freedom is more common in patients with predominantly increased connectivity at the resection region (mean voxel t -score > 0.2 , $n = 24$) compared to those with neutral ($-0.2 < t < 0.2$, $n = 15$) or decreased ($t < 0.2$, $n = 23$) connectivity ($\chi^2 = 8.5$, $P = 0.015$, all 61 patients). Results reflect regional connectivity between the resection region and the rest of the brain, compared to corresponding voxels in the non-epileptogenic hemisphere.

we found the frequency of consciousness-impairing seizures, but not consciousness-sparing seizures, to be related to long-range interictal connectivity decreases. This observation is in line with previous studies of ictal network dysfunction in MTLE patients, in which consciousness-impairing seizures are associated with depressed fronto-parietal cortical function (characterized by sleep-like activity on EEG and reduced cerebral blood flow), while neocortical function appears relatively spared during consciousness-sparing seizures (Blumenfeld *et al.*, 2004a, b; Englot *et al.*, 2010). Unique pathophysiological network effects have also been observed in rodents during seizures that cause transient behavioural arrest (Englot *et al.*, 2008, 2009). Overall, there is compelling evidence that focal epilepsy leads to long-range network dysfunction, both during and between seizures.

In our regional connectivity map analyses, postoperative seizure freedom was more common in patients with increased connectivity at the resection site compared to those with decreased connectivity. Why are patients with decreased connectivity at the resection region more likely to continue having seizures after surgery? One possible explanation is that increased regional connectivity predicts

accurate localization of the true epileptogenic zone, leading to seizure freedom, while decreased connectivity suggests incorrect or incomplete delineation of the epileptogenic zone, leading to persistent seizures. If this observation is supported by further study, functional connectivity analysis may have a promising role in predicting surgical outcome and confirming localization of the epileptogenic zone during the preoperative epilepsy surgery evaluation.

Interestingly, while increased connectivity at the resection zone may predict favourable seizure outcome in epilepsy patients, we previously reported dissimilar results in the setting of glioma surgery, where increased connectivity predicted poor neurological outcome (Tarapore *et al.*, 2012). Specifically, glioma patients with increased regional connectivity at the area of resection were more likely to experience a new postoperative neurological deficit than those with decreased connectivity. Of note, we did not find an association between connectivity at the resection bed and new neurological deficit in the present study of epilepsy surgery. It is possible that increased regional connectivity in glioma represents the ‘physiological connectivity’ of eloquent cortex infiltrated by tumour, whereas elevated connectivity in epilepsy reflects ‘pathophysiological connectivity’ related to epileptogenic tissue. Future study of RSFC in glioma patients with and without epilepsy may shed more light on this issue.

Limitations related to both our techniques and study design should be addressed. First, given that MEG source localization is more challenging with deeper regions, some have argued that MEG has diminished utility in evaluating subcortical structures, such as the mesial temporal lobe in MTLE (Shigeto *et al.*, 2002; Leijten *et al.*, 2003). Innovative source reconstruction algorithms are rapidly evolving, allowing improved localization of the neural sources underlying electromagnetic signals (Dalal *et al.*, 2008, 2011; Wipf and Nagarajan, 2009; Owen *et al.*, 2012), and previous studies of interictal spike mapping have also demonstrated favourable localization with MEG in MTLE patients (Baumgartner *et al.*, 2000; Stephen *et al.*, 2005; Kaiboriboon *et al.*, 2010; Englot *et al.*, 2015). Nevertheless, further studies validating MEG source modelling of mesial temporal signals will be important going forward, along with continued innovation in reconstruction procedures. Next, given the retrospective nature of our study, possible selection bias must be considered in the interpretation of clinical outcomes, and prospective study of functional connectivity in presurgical epilepsy patients represents a worthwhile future endeavour. Finally, it is important to recognize that epilepsy patients comprise a heterogeneous population, with regard to pathophysiology, location, and extent of the epileptogenic zone, and with respect to the various anti-epileptic medications used to treat seizures. Each patient in our series was taking at least one anti-convulsant agent at the time of recordings, and had tried multiple medication regimens in the past, as is the case in previous studies of functional connectivity in intractable epilepsy. The impacts of anti-epileptic drugs on

functional connectivity are not yet known, and are likely significant. Ethical considerations limit the ability to administer these medications to control subjects, or to discontinue them in epilepsy patients for research purposes. However, medication weaning is often a part of inpatient presurgical video-EEG monitoring, and connectivity analyses of MEG recorded during this time window may be revealing in the future.

Conclusions

Using MEG-based functional connectivity map analysis in focal epilepsy, we observed decreased RSFC in widespread neocortical regions in patients versus controls. Global reductions in functional connectivity were related to epilepsy duration and frequency of consciousness-impairing seizures, and thus may reflect the deleterious long-range effects of seizures on brain networks over time. At the area of resection, however, increased regional connectivity predicted seizure freedom after surgery. Overall, our results suggest that MEG-based RSFC analysis in focal epilepsy may lead to a better understanding of brain network dysfunction in this disorder, and may help guide surgical planning and outcome prediction.

Acknowledgements

We thank all members of the UCSF Comprehensive Epilepsy Centre and the Biomagnetic Imaging Lab for their support of this work, and for continued excellence in patient care.

Funding

This work was supported in part by the National Institutes of Health (F32-NS086353 to D.J.E.; R01-DC013979 and R21-NS76171 to S.S.N.) and the National Science Foundation (BCS-1262297 to S.S.N.).

References

- Bartolomei F, Bettus G, Stam CJ, Guye M. Interictal network properties in mesial temporal lobe epilepsy: a graph theoretical study from intracerebral recordings. *Clin Neurophysiol* 2013; 124: 2345–53.
- Baumgartner C, Pataraja E, Lindinger G, Deecke L. Neuromagnetic recordings in temporal lobe epilepsy. *J Clin Neurophysiol* 2000; 17: 177–89.
- Bettus G, Wendling F, Guye M, Valton L, Regis J, Chauvel P, *et al.* Enhanced EEG functional connectivity in mesial temporal lobe epilepsy. *Epilepsy Res* 2008; 81: 58–68.
- Blumenfeld H, McNally KA, Vanderhill SD, Paige AL, Chung R, Davis K, *et al.* Positive and negative network correlations in temporal lobe epilepsy. *Cereb Cortex* 2004a; 14: 892–902.
- Blumenfeld H, Rivera M, McNally KA, Davis K, Spencer DD, Spencer SS. Ictal neocortical slowing in temporal lobe epilepsy. *Neurology* 2004b; 63: 1015–21.

- Bonilha L, Rorden C, Appenzeller S, Coan AC, Cendes F, Li LM. Gray matter atrophy associated with duration of temporal lobe epilepsy. *Neuroimage* 2006 Sep; 32: 1070–9.
- Burgess RC. Evaluation of brain connectivity: the role of magnetoencephalography. *Epilepsia* 2011; 52 (Suppl 4): 28–31.
- Choi H, Sell RL, Lenert L, Muennig P, Goodman RR, Gilliam FG, et al. Epilepsy surgery for pharmacoresistant temporal lobe epilepsy: a decision analysis. *JAMA* 2008; 300: 2497–505.
- Dalal SS, Guggisberg AG, Edwards E, Sekihara K, Findlay AM, Canolty RT, et al. Five-dimensional neuroimaging: localization of the time-frequency dynamics of cortical activity. *Neuroimage* 2008; 40: 1686–700.
- Dalal SS, Zumer JM, Guggisberg AG, Trumpis M, Wong DD, Sekihara K, et al. MEG/EEG source reconstruction, statistical evaluation, and visualization with NUTMEG. *Comput Intell Neurosci* 2011; 2011: 758973.
- Danielson NB, Guo JN, Blumenfeld H. The default mode network and altered consciousness in epilepsy. *Behav Neurol* 2011; 24: 55–65.
- Diehl B, LaPresto E, Najm I, Raja S, Rona S, Babb T, et al. Neocortical temporal FDG-PET hypometabolism correlates with temporal lobe atrophy in hippocampal sclerosis associated with microscopic cortical dysplasia. *Epilepsia* 2003; 44: 559–64.
- Elliott I, Kadis DS, Lach L, Olds J, McCleary L, Whiting S, et al. Quality of life in young adults who underwent resective surgery for epilepsy in childhood. *Epilepsia* 2012; 53: 1577–86.
- Engel J Jr, Thompson PM, Stern JM, Staba RJ, Bragin A, Mody I. Connectomics and epilepsy. *Curr Opin Neurol* 2013; 26: 186–94.
- Engel J, Van Ness P, Rasmussen T, Ojemann L. Outcome with respect to epileptic seizures. In: Engel J, editor. *Surgical treatment of the rpilepsies*. New York: Raven Press; 1993. p. 609–21.
- Englot DJ, Blumenfeld H. Consciousness and epilepsy: why are complex-partial seizures complex? *Prog Brain Res* 2009; 177: 147–70.
- Englot DJ, Han SJ, Rolston JD, Ivan ME, Kuperman RA, Chang EF, et al. Epilepsy surgery failure in children: a quantitative and qualitative analysis. *J Neurosurg Pediatrics* 2014a; 14: 386–95.
- Englot DJ, Lee AT, Tsai C, Halabi C, Barbaro NM, Auguste KI, et al. Seizure types and frequency in patients who “fail” temporal lobectomy for intractable epilepsy. *Neurosurgery* 2013; 73: 838–44.
- Englot DJ, Mishra AM, Mansuripur PK, Herman P, Hyder F, Blumenfeld H. Remote effects of focal hippocampal seizures on the rat neocortex. *J Neurosci* 2008; 28: 9066–81.
- Englot DJ, Modi B, Mishra AM, DeSalvo M, Hyder F, Blumenfeld H. Cortical deactivation induced by subcortical network dysfunction in limbic seizures. *J Neurosci* 2009; 29: 13006–18.
- Englot DJ, Nagarajan SS, Imber BS, Raygor KP, Honma SM, Mizuiru D, et al. Epileptogenic zone localization using magnetoencephalography predicts seizure freedom in epilepsy surgery. *Epilepsia* 2015. doi: 10.1111/epi.13002.
- Englot DJ, Raygor KP, Molinaro AM, Garcia PA, Knowlton RC, Auguste KI, et al. Factors associated with failed focal neocortical epilepsy surgery. *Neurosurgery* 2014b Dec; 75: 648–56.
- Englot DJ, Yang L, Hamid H, Danielson N, Bai X, Marfeo A, et al. Impaired consciousness in temporal lobe seizures: role of cortical slow activity. *Brain* 2010; 133 (Pt 12): 3764–77.
- Garces P, Vicente R, Wibral M, Pineda-Pardo JA, Lopez ME, Aurteneaxe S, et al. Brain-wide slowing of spontaneous alpha rhythms in mild cognitive impairment. *Front Aging Neurosci* 2013; 5: 100.
- Guggisberg AG, Honma SM, Findlay AM, Dalal SS, Kirsch HE, Berger MS, et al. Mapping functional connectivity in patients with brain lesions. *Ann Neurol* 2008; 63: 193–203.
- Haneef Z, Lenartowicz A, Yeh HJ, Engel J Jr, Stern JM. Network analysis of the default mode network using functional connectivity MRI in Temporal Lobe Epilepsy. *J Vis Exp* 2014a: e51442.
- Haneef Z, Lenartowicz A, Yeh HJ, Levin HS, Engel J Jr, Stern JM. Functional connectivity of hippocampal networks in temporal lobe epilepsy. *Epilepsia* 2014b; 55: 137–45.
- Helmstaedter C, Kockelmann E. Cognitive outcomes in patients with chronic temporal lobe epilepsy. *Epilepsia* 2006; 47 (Suppl 2): 96–8.
- Hermann BP, Seidenberg M, Schoenfeld J, Davies K. Neuropsychological characteristics of the syndrome of mesial temporal lobe epilepsy. *Arch Neurol* 1997; 54: 369–76.
- Hinkley LB, Marco EJ, Findlay AM, Honma S, Jeremy RJ, Strominger Z, et al. The role of corpus callosum development in functional connectivity and cognitive processing. *PLoS One* 2012; 7: e39804.
- Hinkley LB, Vinogradov S, Guggisberg AG, Fisher M, Findlay AM, Nagarajan SS. Clinical symptoms and alpha band resting-state functional connectivity imaging in patients with schizophrenia: implications for novel approaches to treatment. *Biol Psychiatry* 2011; 70: 1134–42.
- Holmes M, Folley BS, Sonmezurk HH, Gore JC, Kang H, Abou-Khalil B, et al. Resting state functional connectivity of the hippocampus associated with neurocognitive function in left temporal lobe epilepsy. *Hum Brain Mapp* 2014; 35: 735–44.
- Hyder F, Rothman DL. Quantitative fMRI and oxidative neuroenergetics. *Neuroimage* 2012; 62: 985–94.
- Jeong W, Jin SH, Kim M, Kim JS, Chung CK. Abnormal functional brain network in epilepsy patients with focal cortical dysplasia. *Epilepsy Res* 2014; 108: 1618–26.
- Jiruska P, de Curtis M, Jefferys JG, Schevon CA, Schiff SJ, Schindler K. Synchronization and desynchronization in epilepsy: controversies and hypotheses. *J Physiol* 2013; 591: 787–97.
- Kaiboriboon K, Nagarajan S, Mantle M, Kirsch HE. Interictal MEG/MSI in intractable mesial temporal lobe epilepsy: spike yield and characterization. *Clin Neurophysiol* 2010; 121: 325–31.
- Larsson PG, Kostov H. Lower frequency variability in the alpha activity in EEG among patients with epilepsy. *Clin Neurophysiol* 2005; 116: 2701–6.
- Laurent A, Arzimanoglou A. Cognitive impairments in children with nonidiopathic temporal lobe epilepsy. *Epilepsia* 2006; 47 (Suppl 2): 99–102.
- Leijten FS, Huiskamp GJ, Hilgersom I, Van Huffelen AC. High-resolution source imaging in mesiotemporal lobe epilepsy: a comparison between MEG and simultaneous EEG. *J Clin Neurophysiol* 2003; 20: 227–38.
- Liao W, Zhang Z, Pan Z, Mantini D, Ding J, Duan X, et al. Altered functional connectivity and small-world in mesial temporal lobe epilepsy. *PLoS One* 2010; 5: e8525.
- Luo C, An D, Yao D, Gotman J. Patient-specific connectivity pattern of epileptic network in frontal lobe epilepsy. *Neuroimage Clin* 2014; 4: 668–75.
- Luo C, Qiu C, Guo Z, Fang J, Li Q, Lei X, et al. Disrupted functional brain connectivity in partial epilepsy: a resting-state fMRI study. *PLoS One* 2011; 7: e28196.
- Macrodimitris S, Sherman EM, Williams TS, Bigras C, Wiebe S. Measuring patient satisfaction following epilepsy surgery. *Epilepsia* 2011; 52: 1409–17.
- Maneshi M, Vahdat S, Fahoum F, Grova C, Gotman J. Specific resting-state brain networks in mesial temporal lobe epilepsy. *Front Neurol* 2014; 5: 127.
- Martino J, Honma SM, Findlay AM, Guggisberg AG, Owen JP, Kirsch HE, et al. Resting functional connectivity in patients with brain tumors in eloquent areas. *Ann Neurol* 2011; 69: 521–32.
- Nolte G, Bai O, Wheaton L, Mari Z, Vorbach S, Hallett M. Identifying true brain interaction from EEG data using the imaginary part of coherency. *Clin Neurophysiol* 2004; 115: 2292–307.
- Owen JP, Sekihara K, Nagarajan SS. Non-parametric statistical thresholding for sparse magnetoencephalography source reconstructions. *Front Neurosci* 2012; 6: 186.
- Sekihara K, Hild KE, 2nd, Nagarajan SS. A novel adaptive beamformer for MEG source reconstruction effective when large background brain activities exist. *IEEE Trans Biomed Eng* 2006; 53: 1755–64.

- Sekihara K, Owen JP, Trisno S, Nagarajan SS. Removal of spurious coherence in MEG source-space coherence analysis. *IEEE Trans Biomed Eng* 2011; 58: 3121–9.
- Shigeto H, Morioka T, Hisada K, Nishio S, Ishibashi H, Kira D, et al. Feasibility and limitations of magnetoencephalographic detection of epileptic discharges: simultaneous recording of magnetic fields and electrocorticography. *Neurol Res* 2002; 24: 531–6.
- Spencer S, Huh L. Outcomes of epilepsy surgery in adults and children. *Lancet Neurol* 2008; 7: 525–37.
- Stefan H, Rampp S, Knowlton RC. Magnetoencephalography adds to the surgical evaluation process. *Epilepsy Behav* 2011; 20: 172–7.
- Stephen JM, Ranken DM, Aine CJ, Weisend MP, Shih JJ. Differentiability of simulated MEG hippocampal, medial temporal and neocortical temporal epileptic spike activity. *J Clin Neurophysiol* 2005; 22: 388–401.
- Tarapore PE, Findlay AM, Lahue SC, Lee H, Honma SM, Mizuiri D, et al. Resting state magnetoencephalography functional connectivity in traumatic brain injury. *J Neurosurg* 2013; 118: 1306–16.
- Tarapore PE, Martino J, Guggisberg AG, Owen J, Honma SM, Findlay A, et al. Magnetoencephalographic imaging of resting-state functional connectivity predicts postsurgical neurological outcome in brain gliomas. *Neurosurgery* 2012; 71: 1012–22.
- van Dellen E, Douw L, Hillebrand A, de Witt Hamer PC, Baayen JC, Heimans JJ, et al. Epilepsy surgery outcome and functional network alterations in longitudinal MEG: a minimum spanning tree analysis. *Neuroimage* 2014; 86: 354–63.
- Voets NL, Beckmann CF, Cole DM, Hong S, Bernasconi A, Bernasconi N. Structural substrates for resting network disruption in temporal lobe epilepsy. *Brain* 2012; 135 (Pt 8): 2350–7.
- Wipf D, Nagarajan S. A unified Bayesian framework for MEG/EEG source imaging. *Neuroimage* 2009; 44: 947–66.
- Wu T, Ge S, Zhang R, Liu H, Chen Q, Zhao R, et al. Neuromagnetic coherence of epileptic activity: an MEG study. *Seizure* 2014; 23: 417–23.
- Yuan J, Chen Y, Hirsch E. Intracranial electrodes in the presurgical evaluation of epilepsy. *Neurol Sci* 2012; 33: 723–9.
- Zaveri HP, Pincus SM, Goncharova, II, Duckrow RB, Spencer DD, Spencer SS. Localization-related epilepsy exhibits significant connectivity away from the seizure-onset area. *Neuroreport* 2009; 20: 891–5.
- Zhang Z, Liao W, Chen H, Mantini D, Ding JR, Xu Q, et al. Altered functional-structural coupling of large-scale brain networks in idiopathic generalized epilepsy. *Brain* 2011; 134 (Pt 10): 2912–28.
- Zhang Z, Lu G, Zhong Y, Tan Q, Liao W, Wang Z, et al. Altered spontaneous neuronal activity of the default-mode network in mesial temporal lobe epilepsy. *Brain Res* 2010; 1323: 152–60.